

Received: 2018.04.01

Accepted: 2018.05.07

Published: 2018.05.21

Magnolol and Honokiol Attenuate Apoptosis of Enterotoxigenic *Escherichia Coli*-Induced Intestinal Epithelium by Maintaining Secretion and Absorption Homeostasis and Protecting Mucosal Integrity

Authors' Contribution:

Study Design A
Data Collection B
Statistical Analysis C
Data Interpretation D
Manuscript Preparation E
Literature Search F
Funds Collection G

ABDEF 1,2

Yanli Deng

A 3 **Xuefeng Han**

CD 3 **Shaoxun Tang**

A 4 **Chengjian Li**

AG 1 **Wenjun Xiao**

AG 3 **Zhiliang Tan**

1 National Research Center of Engineering Technology for Utilization of Botanical Functional Ingredients, Hunan Agricultural University, Hunan Collaborative Innovation Center for Utilization of Botanical Functional Ingredients, Changsha, Hunan, P.R. China

2 Tea College of Guizhou University, Guiyang, Guizhou, P.R. China

3 Key Laboratory for Agro-Ecological Processes in Subtropical Region, and South-Central Experimental Station of Animal Nutrition and Feed Science in Ministry of Agriculture, Institute of Subtropical Agriculture, Chinese Academy of Sciences, Changsha, Hunan, P.R. China

4 Department of Pharmacy, Yongzhou Vocational Technical College, Yongzhou, Hunan, P. R. China

Corresponding Authors:

Wenjun Xiao, e-mail: xiaowenjun88@sina.com, Zhiliang Tan, e-mail: zltan@isa.ac.cn

Source of support:

This study was financially supported by the National Natural Science Foundation of China (Grant number 30972166), Hunan Provincial Graduate Student Innovation Conditions (Grant number CX2011B304, CX2014B300), Hunan Provincial Science and Key Technology Project (Grant number 2017NK1020), and Hunan Provincial Natural Science Foundation of China (Grant number 2018JJ5052)

Background:

The cortex of *Magnolia officinalis* has long been used as an element of traditional Chinese medicine for the treatment of anxiety, chronic bronchitis, and gastrointestinal dysfunction. This study aimed to elucidate the underlying mechanism of its functional ingredients (magnolol and honokiol) in modifying the secretion and absorption homeostasis and protecting mucosal integrity in an *Enterotoxigenic Escherichia coli* (ETEC)-induced diarrhea mouse model.

Material/Methods:

This study established a diarrhea mouse model infected by ETEC at a dosage of 0.02 ml/g live body weight (BW) *in vivo*. Magnolol or honokiol was followed by an intraperitoneal administration at dosages of 100, 300, and 500 mg/kg BW according to a 3×3 factorial arrangement. The useful biomarkers for evaluating the integrity of intestinal tract and histologic injury were analyzed and morphological development (including villus height, crypt depth, and ratio of villus height to crypt depth) and the expressions of inflammatory cytokines were determined by real-time PCR.

Results:

The results showed that magnolol and honokiol (500 mg/kg BW) reduced the concentrations of NO, DAO, and DLA, and iNOS activity, and the mRNA expressions of the interferon gamma (IFN-γ) and interleukin 10 (IL-10), and inhibited intestinal epithelial cell apoptosis. Magnolol and honokiol (300 mg/kg BW) elongated the villus height and crypt depth and decreased the number of goblet cells and the ratio of villus height to crypt depth.

Conclusions:

The current results indicate that magnolol and honokiol enhance the intestinal anti-inflammatory capacities, elongate the villus height and crypt depth, and reduce goblet cell numbers to inhibit the intestinal epithelium apoptosis and effectively protect the intestinal mucosa. These results show that magnolol and honokiol protect the intestinal mucosal integrity and regulate gastrointestinal dysfunction.

MeSH Keywords:

Apoptosis • Enterotoxigenic *Escherichia coli* • Intestinal Mucosa • Magnolia

Full-text PDF:

<https://www.medscimonit.com/abstract/index/idArt/910350>

 3014

 6

 2

 29



Background

Enterotoxigenic *Escherichia coli* (ETEC) is an enteric pathogen that easily causes secretory diarrhea and death in animals and humans due to the activities of enterotoxins [1]. The enteric pathogen often induces programmed cell death or apoptosis in host cells and tissues to promote their survival and dissemination during infection [2, 3]. A prior study reported that ETEC infection rapidly induced the loss of plasma membrane asymmetry of porcine intestinal epithelial cells and reduced the cell metabolic activity via activating caspase 3, and camptothecin-induced apoptosis in the epithelial cells promoted subsequent ETEC adherence [2]. Other studies have proven that enterotoxin can alter the intestinal tight junction and permeability [4], causing break-down of the cytoskeleton [5], resulting in severe villus atrophy and crypt hypoplasia inside the enterocytes [6]. The villus atrophy and crypt hypertrophy adversely alter the balance between absorptive and secretory cells, and the inflammatory response generates secretion-stimulating inflammatory mediators that worsen diarrhea, further inducing the apoptotic program that accompanies diseases such as gastritis, colitis, and cancer [7].

Magnolia officinalis cortex (MOC) is a traditional Chinese medicine for symptomatic treatment of gastrointestinal disorders. Magnolol and honokiol are the main bioactive compounds isolated from MOC, with a number of diverse pharmacological functions, including antioxidation [8], anti-bacteria [9], anti-proliferation [10], and anti-gastric effects [11]. Magnolol and honokiol may regulate the serotonergic and gastroenteric systems [12]. In addition, it has been demonstrated that magnolol differentially regulates spontaneous gastrointestinal motility according to activation of the acetylcholine and 5-hydroxytryptamine receptors in the gastrointestinal tract [13]. Our previous work shows that magnolol and honokiol regulate the calcium-activated potassium channels to elevate the serum concentrations of Cl^- and K^+ , which are mostly associated with attenuation of secretion and promotion of absorption in enterocytes of the small intestine to control diarrhea [14]. The intestinal development responds to digestion and absorption of various nutrients through the intestinal villus and crypt [15]. Therefore, we hypothesized that magnolol and honokiol play an important role in regulating gastroenterology disorders linked with the morphological structure of villus and crypt in intestinal mucosa of ETEC-induced diarrhea mice.

Material and Methods

Animals and experimental design

This study was carried out in strict accordance with the recommendations in the Animal Care and the Use Guidelines of

the Institute of Subtropical Agriculture (ISA) of the Chinese Academy of Sciences. The protocol was approved by the Animal Care Committee on the Ethics of Animal Experiments of ISA (Permit Number: SYXK2015-0189).

The Chinese Kunming mouse strain (*Mus musculus* Km, KM), an outbred mouse strain originating from the Swiss albino mouse, is widely used in pharmacology and genetics studies throughout China. It exhibits many advantages such as high disease resistance, large and frequent litters, and rapid growth rates. Our pre-experimental results show these mice are easily infected by ETEC, so we selected the Chinese Kunming mouse strain as a model mouse. We obtained 120 male Kunming mice 7 weeks old and weighing 25–27 g from the Hunan SLAC Laboratory Animal Company (Changsha, China). The animals were housed individually in a pathogen-free mouse colony (room temperature=22±2°C; relative humidity=45–60%, lighting cycle=12 h light and 12 h dark) with free access to food and water. A diarrhea mouse model was established according to previously described procedures [14]. Briefly, the mice were fasted for 6 h after feeding 3 days for acclimation, then randomly assigned into 12 groups: (1) normal control group (NC), (2) diarrhea model control group (MC), (3) positive drug control group (PC), (4) plant extract group 1, (5) plant extract group 2, (6) plant extract group 3, (7) plant extract group 4, (8) plant extract group 5, (9) plant extract group 6, (10) plant extract group 7, (11) plant extract group 8, and (12) plant extract group 9; details are shown in Table 1. In MC, PC, and 9 plant extract-treated groups, mice received oral administration of 0.02 ml/g body weight (BW) of the prepared ETEC suspensions (3.29×10^9 CFU/ml). NC mice were administered 0.02 ml/g BW sterile water. Three hours later, the diarrhea model was established according to previously described procedures [14]. After that, the NC and MC mice were administered 500 mg/kg BW sterile water. The PC mice were orally gavaged with loperamide hydrochloride at a dosage of 3 mg/kg BW. The 9 plant extract-treated groups were administered magnolol or honokiol at the dosages of 100 (M100 or H100), 300 (M300 or H300), and 500 (M500 or H500) mg/kg BW according to a 3×3 factorial arrangement. All animals were killed by sodium pentobarbital anesthesia (50 mg/kg i.p.) after 5 h of every treatment.

Chemicals and reagents

Loperamide hydrochloride was purchased from Xi'an-Janssen Pharmaceutical Ltd. (Xi'an, China) and dissolved in a 2% Tween 80 solution (0.1875 mg/ml) for oral gavage administration. The ETEC strain O78: K80 suspensions were acquired from our previous study [14]. The ETEC suspensions were grown overnight from the frozen glycerol stocks at 180 rpm and 37°C for 12 h. The cell density of ETEC suspensions was 3.29×10^9 CFU/ml measured by ND-1000 uv-vis spectrophotometer (NanoDrop Ltd., TX).

Table 1. Experimental treatments.

Groups	Group description	Treatments design
Group 1	Normal control group (NC)	All mice were treated with sterile water
Group 2	Diarrhea model control group (MC)	All mice were infected by ETEC
Group 3	Positive drug control group (PC)	All mice were infected by ETEC, and then were orally gavaged with loperamide hydrochloride 3 mg/kg BW
Group 4	Plant extract group 1	All mice were infected by ETEC, and then were administered the magnolol 100 mg/kg BW and honokiol 100 mg/kg BW
Group 5	Plant extract group 2	All mice were infected by ETEC, and then were administered the magnolol 100 mg/kg BW and honokiol 300 mg/kg BW
Group 6	Plant extract group 3	All mice were infected by ETEC, and then were administered the magnolol 100 mg/kg BW and honokiol 500 mg/kg BW
Group 7	Plant extract group 4	All mice were infected by ETEC, and then were administered the magnolol 300 mg/kg BW and honokiol 100 mg/kg BW
Group 8	Plant extract group 5	All mice were infected by ETEC, and then were administered the magnolol 300 mg/kg BW and honokiol 300 mg/kg BW
Group 9	Plant extract group 6	All mice were infected by ETEC, and then were administered the magnolol 300 mg/kg BW and honokiol 500 mg/kg BW
Group 10	Plant extract group 7	All mice were infected by ETEC, and then were administered the magnolol 500 mg/kg BW and honokiol 100 mg/kg BW
Group 11	Plant extract group 8	All mice were infected by ETEC, and then were administered the magnolol 500 mg/kg BW and honokiol 300 mg/kg BW
Group 12	Plant extract group 9	All mice were infected by ETEC, and then were administered the magnolol 500 mg/kg BW and honokiol 500 mg/kg BW

Magnolol and honokiol were extracted from MOC and separated and purified according to the methods described in our previous experiment [14]. The purity of magnolol and honokiol was determined by high-performance liquid chromatography (HPLC) analysis (Fisher Chemical, Loughborough, UK) as follows: the column used in the present study was a Kromasil C18 column (4.6×200 mm I.D., 5 µm, Waters Thermo), the mobile phase composed of methanol-water (80: 20, v/v) was eluted at a flow-rate of 1.0 mL/min and the UV detector was set at 294 nm, and the temperature was set at 40°C. The extracted magnolol and honokiol purity was above 98% and dissolved in a 2% Tween 80 solution for oral gavage administration.

Assessment on chemical biomarkers

The blood samples were centrifuged (3500×g for 10 min) to separate the serum, then stored at -80°C until analysis. The serum glucose (GLU) and D-lactic acid (DLA) concentration in the serum were analyzed using commercial kits (Beijing Leadman Biochemistry Co., Ltd., Beijing, China) in accordance with the manufacturer's instructions. The ileum tissue was immediately homogenized with cold 0.9% sterile saline on ice, then centrifuged at 3500×g for 15 min to get the resultant liquid

supernatant. The serum diamine oxidase (DAO) concentration and the nitric oxide (NO) and induced nitric oxide synthase (iNOS) concentrations of homogenized solution were determined by the assay kits (Nanjing Jiancheng Bioengineering Institute, Nanjing, China) colorimetrically with a UV 8500 II spectrophotometer (Thermo Electron Corporation, Rochester, NY, USA).

Quantitative real-time polymerase chain reaction (qRT-PCR) assay

Total RNA was isolated from the liquid nitrogen-frozen ileum tissue using TRIZOL reagents (Invitrogen, USA) and cDNA was generated using the RevertAid™ First Strand cDNA Synthesis Kit from Fermentas (Fermentas Inc., Ontario, Canada), according to the manufacturer's instructions. Oligonucleotide primers according to the mouse gene sequence (<http://www.ncbi.nlm.nih.gov/pubmed/>) were designed for the genes in Table 2 using Primer 5 software (Premier Co., Canada). Then, qRT-PCR analyses were performed on the aliquots of the cDNA preparations with Power SYBR Green PCR Master Mix (Applied Biosystems Inc., Foster City, CA, USA) to quantitatively detect the mRNA expression of genes described in Table 2 and β-actin

Table 2. Sequences of primers and PCR products size of real-time quantitative PCR.

Gene*	GenBank accession	Forward primer (5'-3')	Reverse primer (5'-3')	Product size (bp)
β-actin	NM_007393	AGAGGGAAATCGTGCCTGAC	CAATAGTGATGACCTGGCCGT	139
TNF-α	NM_013693	CATCTTCTCAAATTCGAGTGACAA	TGGGAGTAGACAAGGTACAACCC	175
IFN-γ	NM_008337	TCAAGTGGCATAGATGTGGAAGAA	TGGCTCTGCAGGATTTTCATG	92
IL-6	NM_031168	GAGGATACCACTCCCAACAGACC	AAGTGCATCATCGTTGTTTCATACA	141
IL-10	NM_010548	GGTTGCCAAGCCTTATCGGA	ACCTGC CCACTGCCTTGCT	190
iNOS	NM_010927	CAGCTGGGCTGTACAAACCTT	ATTGGAAGTGAAGCGTTTCG	94

* TNF-α – tumor necrosis factor alpha; IFN-γ – interferon gamma; IL-6 – interleukin 6; IL-10 – interleukin 10; iNOS – inducible nitric oxide synthase.

(as an internal standard) using the Applied Biosystems 7900 Fast Real-Time PCR System (Applied BioSystems Inc., Foster City, CA, USA). All assays were validated using melting curve by the presence of single PCR products. The program for PCR reactions was 95°C for 10 min followed by 40 cycles of 95°C for 15 s and 60°C for 60 s. At the end of real-time PCR, the threshold cycle value (CT) of each reaction was determined. The change in transcriptional level of target gene normalized to β-actin was calculated by the following formula: Relative mRNA level of target gene (fold of control) = $2^{-\Delta\Delta CT}$. In the current experiment, $-\Delta\Delta CT = -(\Delta CT \text{ experiment group} - \Delta CT \text{ control group})$ and $\Delta CT = CT \text{ samples} - CT \beta\text{-actin}$.

Histological evaluation

At 5 h after administration of magnolol and honokiol, the mice were killed by sodium pentobarbital anesthesia. The ileum segments from 5 animals/group were removed for histopathological analysis and fixed overnight in 4% buffered paraformaldehyde at 4°C. Then, the sections were rinsed in water, dehydrated by immersion in increasing ethanol concentrations (75%, 85%, 95%, 100%), cleared in benzene, and saturated and embedded with paraffin. After a routine process including fixation, dehydration, hyalinization, and paraffin embedding, the ileum segments were sectioned at 5-μm thickness (10 slices per sample) and placed on slides. The slides were dewaxed, hydrated, and then stained with hematoxylin and eosin and viewed under a light Olympus BH-2 microscope (Olympus BH-2, Olympus, Tokyo, Japan). The lengths of 30 villi were measured by the distance in μm from the crypt neck to the villus tip, and the depths of 30 crypts were determined using the Image C picture analysis system (Intronic GmbH, Berlin, Germany). The goblet cells numbers in each 30 oriented villi were counted and coupled to the Image C picture analysis system (Intronic GmbH, Berlin, Germany).

Terminal deoxynucleotidyl transferase mediated dUTP nick-end labeling (TUNEL) assay

The ileum sections were obtained as described above. The TUNEL staining was performed to detect the apoptotic cells using the In Situ Cell Death Detection Kit (Nanjing KeyGEN Biotech. Co., Ltd., Nanjing, Jiangsu, China) according to the manufacturer's instruction. Images of TUNEL staining were made using an Olympus BH-2 microscope (Beckman Coulter, Inc., CA, USA). Apoptosis was quantified by analysis of the integrated average optical density of TUNEL staining images.

Statistical analyses

Data, not including MC, PC, and NC groups, were statistically analyzed using the procedures of SAS (8.2) software (2000; SAS Inc., Cary, NC, USA). The model included the fixed effects of magnolol, honokiol, and magnolol × honokiol with the animal as the random effect. All data (including MC, PC, and NC groups) were subsequently examined to compare the treatment differences by using the General Linear Models procedure of SAS (8.2), and the statistical model only included the fixed effects of treatments. Least-squares means were reported throughout, and differences at $P < 0.05$ were considered statistically significant.

Results

The purity of magnolol and honokiol used in this study was 98% as determined by HPLC. Table 3 shows that magnolol administration affected ($P < 0.05$) the levels of iNOS, DAO, and DLA in a dose-dependent manner, while honokiol administration affected ($P < 0.05$) the concentrations of NO and GLU and the activity of iNOS. There were interactive effects of magnolol and honokiol on the generation of NO and DLA ($P < 0.001$), and iNOS and GLU ($P < 0.05$). Compared with the NC group, intraperitoneal administration of ETEC increased ($P < 0.05$) the

Table 3. Effects of oral magnolol and honokiol administration on NO and iNOS concentration of ileal tissue, serum DAO, GLU, and LAD content in mice (n=10).

Item*		Treatment**									SEM#	P-value		
		NC	MC	PC	M			H				M	H	M×H
					100	300	500	100	300	500				
Ileum	NO μmol/g prot	3.11 ^c	11.28 ^a	3.79 ^c	5.75 ^{bc}	5.73 ^{bc}	5.01 ^{bc}	9.20 ^{ab}	7.67 ^{abc}	5.32 ^{bc}	2.329	0.661	0.041	<0.001
	iNOS U/mg prot	0.73 ^{abcd}	0.92 ^a	0.89 ^a	0.75 ^{abc}	0.54 ^{cde}	0.39 ^e	0.81 ^{ab}	0.59 ^{bcde}	0.49 ^{de}	0.109	<0.010	0.003	0.012
Serum	DAO U/L	3.73 ^{abc}	4.32 ^{ab}	4.54 ^a	3.73 ^{abc}	3.41 ^{bc}	3.18 ^c	4.21 ^{ab}	3.60 ^{bc}	3.64 ^{abc}	0.396	0.046	0.099	0.996
	GLU mmol/L	5.04 ^b	5.75 ^{ab}	5.93 ^{ab}	6.07 ^{ab}	6.42 ^{ab}	5.66 ^{ab}	4.89 ^b	7.20 ^a	6.08 ^{ab}	0.924	0.556	0.006	0.008
	DLA mg/dL	40.95 ^b	77.80 ^a	36.54 ^{bc}	34.06 ^{bc}	29.05 ^c	35.05 ^{bc}	30.51 ^c	32.81 ^c	34.42 ^{bc}	3.526	0.038	0.139	<0.001

* NO – nitric oxide; iNOS – induced nitric oxide synthase; DAO – diamine oxidase; GLU – glucose; DLA – lactic acid. ** In a row, the mean values with different letters (a–e) differ ($P<0.05$). NC – normal control; MC – diarrhea model control; PC – positive drug control; M – magnolol administration at the doses of 100, 300, and 500 mg/kg BW; H – Honokiol administration at the doses of 100, 300, and 500 mg/kg BW. # Standard error of least squares means.

Table 4. Effects of oral magnolol and honokiol administration on the mRNA expression of nitric oxide synthases and inflammatory cytokines in mice (n=10).

Item*		Treatment**									SEM#	P-value		
		NC	MC	PC	M			H				M	H	M × H
					100	300	500	100	300	500				
iNOS		1.00 ^b	1.88 ^{ab}	2.60 ^a	1.64 ^b	1.37 ^b	1.01 ^b	1.64 ^b	1.60 ^b	1.25 ^b	0.443	0.004	0.214	<0.001
TNF-α		1.00	1.74	1.54	1.43	1.18	1.09	1.27	0.89	1.06	0.386	0.418	0.049	0.004
IFN-γ		1.00 ^c	2.08 ^a	1.53 ^{abc}	1.99 ^{ab}	0.89 ^c	0.78 ^c	1.51 ^{abc}	1.21 ^{bc}	1.06 ^c	0.366	<0.001	0.081	<0.001
IL-6		1.00 ^{ab}	1.29 ^{ab}	0.60 ^b	1.38 ^a	0.93 ^{ab}	0.82 ^{ab}	1.26 ^{ab}	1.08 ^{ab}	0.78 ^{ab}	0.310	0.018	0.071	0.001
IL-10		1.00 ^d	4.04 ^a	2.63 ^{abc}	3.12 ^{ab}	2.21 ^{bcd}	0.74 ^d	2.73 ^{ab}	2.10 ^{bcd}	1.17 ^{cd}	0.691	<0.001	<0.001	<0.001

* iNOS – nitric oxide synthases; TNF-α – tumor necrosis factor alpha; IFN-γ – interferon gamma; IL-6 – interleukin 6; IL-10 – interleukin 10. ** In a row, the mean values with different letters (a–d) differ ($P<0.05$). NC – normal control; MC – diarrhea model control; PC – positive drug control; M – magnolol administration at the doses of 100, 300, and 500 mg/kg BW; H – Honokiol administration at the doses of 100, 300, and 500 mg/kg BW. # Standard error of least squares means.

concentrations of NO and DLA in the ileum. Administration with loperamide hydrochloride reduced ($P<0.05$) NO and DLA in the PC group compared with the MC group. When compared with the MC group, all doses of magnolol and 500 mg honokiol/kg BW reduced ($P<0.05$) NO, while administration of 300 or 500 mg magnolol and honokiol/kg BW inhibited ($P<0.05$) the activity of iNOS. The activity of DAO was decreased ($P<0.05$) after administration of 500 mg magnolol/kg BW compared with the MC group. Meanwhile, the concentration of DLA was decreased ($P<0.05$) by administration of all doses of magnolol and honokiol in comparison with the MC group.

To further understand the molecular mechanism by which magnolol and honokiol block various inflammatory processes induced by ETEC, the mRNA expression of iNOS, TNF-α, IFN-γ, IL-6, and IL-10 in the ileal tissues of mice were investigated (Table 4). The magnolol administration influenced the mRNA expression of IFN-γ and IL-10 ($P<0.001$), and iNOS and IL-6 ($P<0.05$) in a dose-dependent manner. The honokiol administration had significant effects on the mRNA expression of TNF-α ($P=0.009$) and IL-10 ($P<0.001$) in a dose-dependent manner. There were interactive effects ($P<0.05$) of magnolol and honokiol on the mRNA expression of iNOS, IFN-γ, IL-10 TNF-α, and IL-6. When compared with NC, intraperitoneal

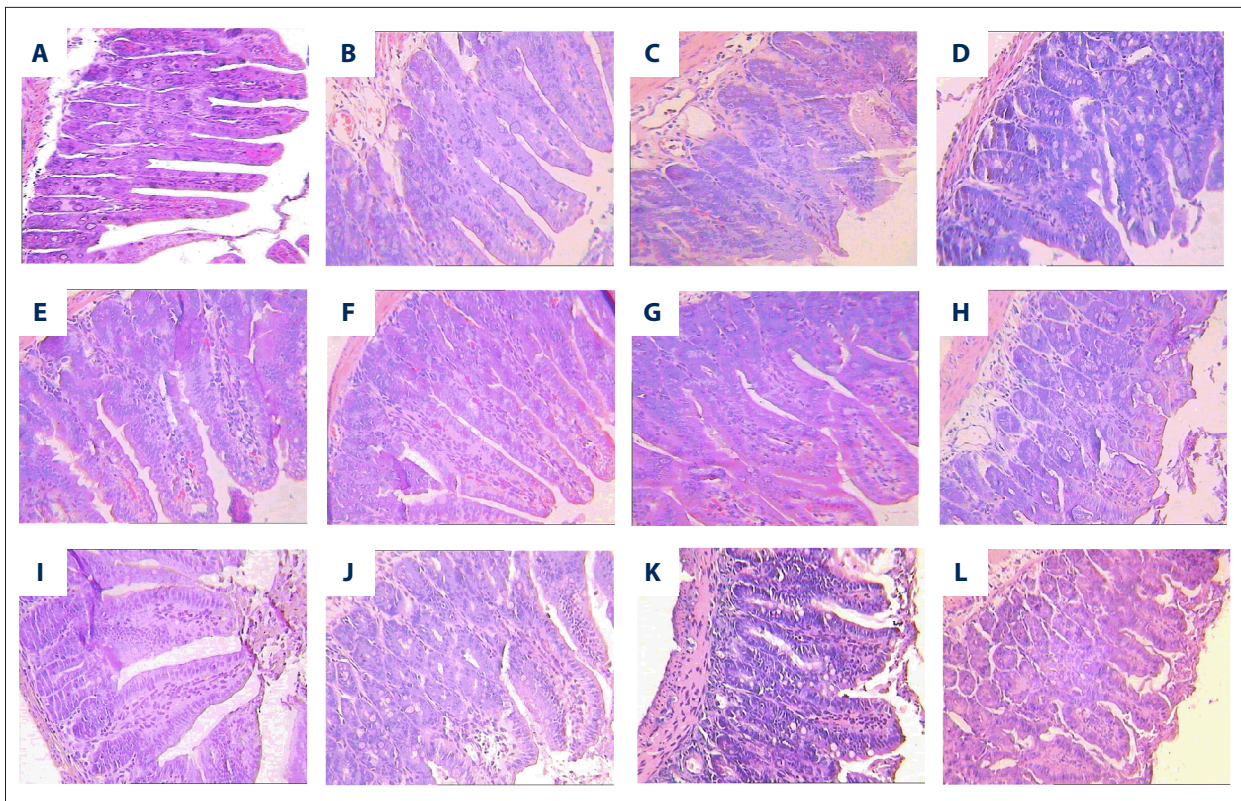


Figure 1. Effects of magnolol and honokiol on ETEC-induced changes in histopathology of the ileal tissue in mice of different experimental groups (n=5, ×250). The lengths of 30 villi were measured by the distance in μm from the crypt neck to the villus tip, the depths of 30 crypts were determined, and the goblet cells in each 30 oriented villi were counted. The mice were first infected by ETEC suspensions and then treated by loperamide hydrochloride or magnolol and honokiol. (A) Shows the normal appearance of normal control mice. (B) Shows the appearance of ETEC-induced mice. (C) Shows the appearance of loperamide hydrochloride-treated ETEC-induced mice. (D–L) Shows the appearance of 100 mg magnolol/kg BW (M100) ×100 mg honokiol/kg BW (H100) administration, M100×H300, M100×H500, M300×H100, M300×H300, M300×H500, M500×H100, M500×H300, and M500×H500 treated ETEC-induced mice.

administration of ETEC increased ($P<0.05$) the mRNA expression of IFN- γ and IL-10. Administration with loperamide hydrochloride had an inhibitory effect on inflammation in comparison with the MC group. When compared with the MC group, the mRNA expression of IFN- γ and IL-10 was markedly inhibited ($P<0.05$) by magnolol and honokiol administration at the doses of 300 and 500 mg/kg BW. Meanwhile, administration with magnolol or honokiol suppressed the mRNA expression of iNOS, TNF- α , and IL-6.

The effects of magnolol and honokiol on the ileal morphology in ETEC-induced mice are presented in Figure 1 and Table 5. After statistical analysis (showed in Table 4), the honokiol administration affected ($P<0.05$) the villus height and the ratio of villus height to crypt depth in a dose-dependent manner. When compared with the NC group, intraperitoneal administration of ETEC decreased ($P<0.05$) the ileum villus height and crypt depth. The goblet cell numbers and ratio of villus height to crypt depth were reduced ($P<0.05$) in the PC group

compared with the MC group. When compared with the MC group, all doses of magnolol and honokiol administration decreased ($P<0.05$) the goblet cell numbers and ratio of villus height to crypt depth, but 300 mg honokiol/kg BW administration did not affect ($P>0.05$) the ratio of villus height to crypt depth. We found that 300 mg magnolol, or 100 and 300 mg honokiol/kg BW administration elongated ($P<0.05$) the crypt depth compared with the MC group.

Figure 2A shows no remarkable apoptosis sign except for the death of some program cell of the ileum in normal control group mice. Figure 2B shows the chromatin of intestinal epithelial cells was deeply stained and fragmented, and their nuclei were margined in the ileum of ETEC-induced mice, which was different from the NC group. Figure 2C shows the chromatin of intestinal epithelial cells was slightly stained compared with that in the MC group (Figure 2B). The chromatin of intestinal epithelial cells was also slightly stained in Figure 2D–2L after being treated by magnolol and honokiol administration

Table 5. Effects of oral magnolol and honokiol administration on the morphology of ileal in mice (n=5).

Item*	Treatment**									SEM#	P-value		
	NC	MC	PC	M			H				M	H	M × H
				100	300	500	100	300	500				
VH, μm	344.06 ^a	229.98 ^{bc}	195.56 ^c	271.03 ^{abc}	288.67 ^{ab}	274.37 ^{abc}	284.51 ^{ab}	316.27 ^{ab}	233.28 ^{bc}	37.132	0.830	0.033	0.381
CD, μm	174.02 ^a	108.24 ^b	121.62 ^{ab}	159.09 ^{ab}	167.89 ^a	155.63 ^{ab}	173.59 ^a	170.17 ^a	138.85 ^{ab}	24.638	0.825	0.184	0.185
GC	24.40 ^a	22.40 ^a	12.20 ^b	5.80 ^c	4.63 ^c	6.53 ^{bc}	8.07 ^{bc}	3.83 ^c	5.07 ^c	2.629	0.633	0.107	0.124
VH/CD	2.00 ^{ab}	2.14 ^a	1.69 ^c	1.72 ^c	1.75 ^{bc}	1.81 ^{bc}	1.68 ^c	1.89 ^{abc}	1.71 ^c	0.119	0.598	0.038	0.116

* VH – Villus height; CD – Crypt depth; GC – Goblet cell; VH/CD – ratio of Villus height to Crypt depth; ** In a row, the mean values with different letters (a–c) differ ($P < 0.05$). NC – normal control; MC – diarrhea model control; PC – positive drug control; M – magnolol administration at the doses of 100, 300, and 500 mg/kg BW; H – Honokiol administration at the doses of 100, 300, and 500 mg/kg BW. # Standard error of least squares means.

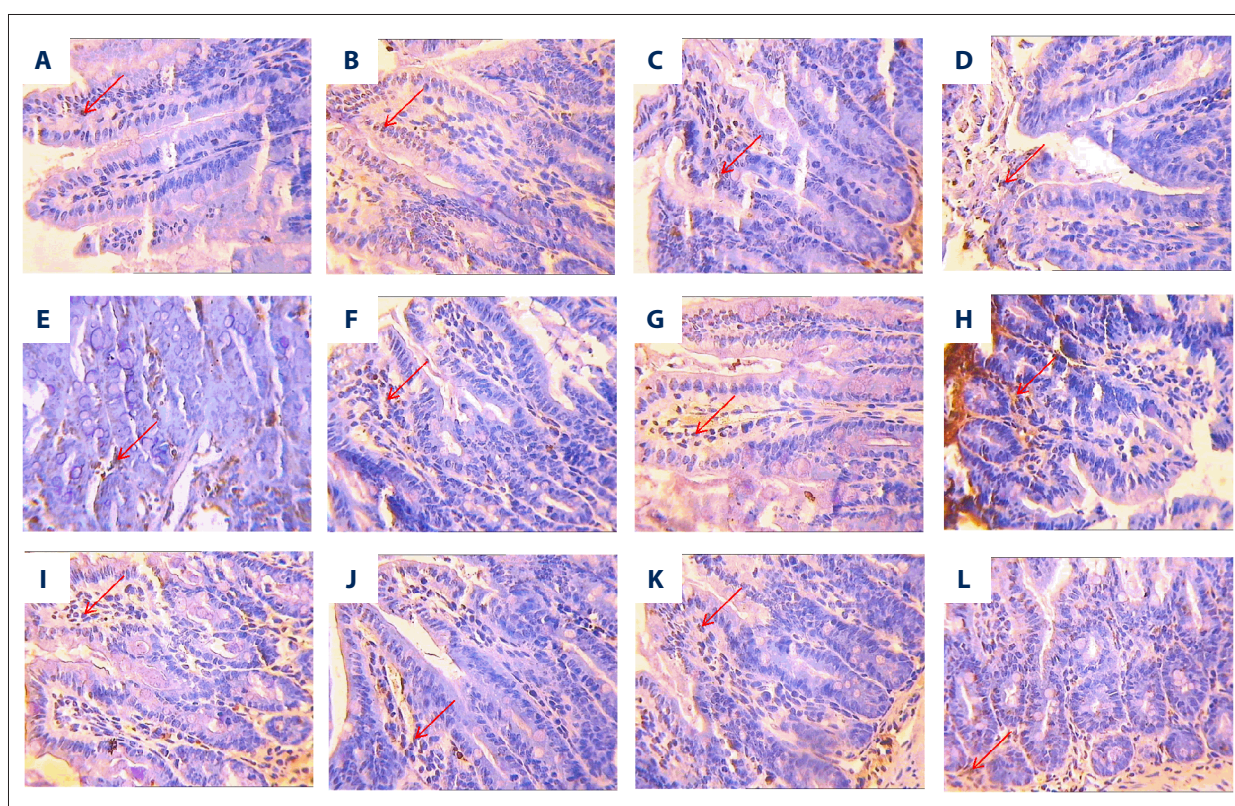


Figure 2. The apoptosis appearance of ETEC-induced ileum tissues treated by magnolol and honokiol in mice of different experimental groups (n=5, ×400). DNA fragmentation was examined by terminal deoxynucleotidyl transferase mediated dUTP nick-end labeling staining. (A) Shows the apoptosis appearance of the normal control mice. (B) Shows the apoptosis appearance of ETEC-induced mice. (C) Shows the apoptosis appearance of loperamide hydrochloride-treated ETEC-induced mice. (D–L) Shows the apoptosis appearance of magnolol and honokiol administration at 100 mg/kg BW (M100) ×100 mg/kg BW (H100), M100×H300, M100×H500, M300×H100, M300×H300, M300×H500, M500×H100, M500×H300, and M500×H500 treated ETEC-induced mice.

in comparison with the MC group. Statistical analysis (Table 6) showed that magnolol administration affected ($P < 0.05$) the average optical density. When compared with the NC group,

intraperitoneal administration of ETEC significantly increased the average optical density. Administration with loperamide hydrochloride reduced ($P < 0.05$) the average optical density

Table 6. Effects of oral magnolol and honokiol administration on the average optical density of ileal epithelium in ETEC-induced diarrhea mice (TUNEL assay, n=5).

Item*	Treatment**									SEM#	P-value		
	NC	MC	PC	M			H				M	H	M × H
				100	300	500	100	300	500				
AID	0.17 ^{ab}	0.20 ^a	0.12 ^b	0.20 ^{ab}	0.16 ^{ab}	0.13 ^{ab}	0.18 ^{ab}	0.15 ^{ab}	0.16 ^{ab}	0.032	0.046	0.500	0.332

* AID – average optical density; ** In a row, the mean values with different letters (a–b) differ significantly ($P < 0.05$). NC – normal control; MC – diarrhea model control; PC – positive drug control; M – magnolol administration at the doses of 100, 300, and 500 mg/kg BW; H – Honokiol administration at the doses of 100, 300, and 500 mg/kg BW; # Standard error of least squares means.

compared with the MC group. When compared with the MC group, magnolol and honokiol administration did not significantly affect ($P > 0.05$) the average optical density.

Discussion

In this study, we focused on the comparison of the MC group and magnolol and honokiol treatments while using NC as a reference. Here, we tried to elucidate the mechanism of magnolol and honokiol in modifying ETEC-induced disruption in ileum intestinal mucosa.

Bacterial pathogens have been reported to invade the intestinal epithelium, reduce cell metabolic activity, and stimulate iNOS over-expression to elevate NO level in diarrhea mice associated with inflamed mucosa [16], which was in agreement with the present results. The significance of NO release is to promote electrolyte (or water) secretion in the ileum of pathological diarrhea mice [16]. In the present study, the magnolol and honokiol administration significantly decreased the NO concentration and iNOS activity, which partly supports the results of previous reports [17,18]. DAO activity and DLA level in serum are useful biomarkers for evaluating the integrity of the gastrointestinal tract and histologic injury [19,20]. In present study, we demonstrated that intraperitoneal administration of ETEC disrupts intestinal function to produce more DAO and DLA in the damaged intestinal mucosal of diarrhea mice, while magnolol and honokiol reduce serum DAO activity and DLA level (Table 2) to protect against mucosal injury. It is thus obvious that magnolol and honokiol have stronger protective effects on intestinal mucosal than that of loperamide hydrochloride.

Secretory diarrhea is a common symptom associated with inflammation of the intestinal mucosa [21]. The data (Table 3) obviously demonstrated that intraperitoneal administration of ETEC promoted the inflammatory process, and we confirmed that severe damage to the intestinal mucosa occurs after ETEC treatment in the ileum of mice. The magnolol and

honokiol administration showed a general tendency to inhibit inflammatory markers iNOS, TNF- α , IFN- γ , IL-6, and IL-10, which is partly in agreement with the findings of previous reports [22,23]. Furthermore, the regulation effects of magnolol and honokiol on inflammation were similar to those of loperamide hydrochloride with the mRNA expression of inflammatory cytokines (iNOS, TNF- α , IFN- γ , IL-6, and IL-10) in MC, PC, and magnolol or honokiol treatment.

The morphology of intestinal mucosa, especially the structure of villus and crypt, is one of the most important indicators of the digestive and absorptive capacity of the small intestine [24]. In the present study, the intestinal injury was evidenced by atrophy of the intestinal villi, reduction of the crypt depth, and decreased numbers of goblet cells in ETEC-induced diarrhea mice, which was supported by previous studies [6,7]. The apoptosis induced by ETEC infection and heat-labile enterotoxin has been observed [25,26], which was partly in agreement with the present results. The villus and crypts affect absorption and secretion, respectively, and the goblet cells located in both regulate the mucus secretion to keep the balance between electrolytes and water in the intestines [27]. Through comparing with ETEC-induced diarrhea mice, we showed that magnolol and honokiol elongated the villus height and crypt depth. A possible explanation is that the elongation of villus height and crypt depth increased absorption capacity to develop intestine morphology, which, based on the elongation of villus height and crypt depth, improve mitotic activity to promote the epithelial cell proliferation to inhibit apoptosis and preserve the integrity of the human epithelial mucosa after bacterial invasion [3]. Intriguingly, the goblet cells depletion and the decreased ratio of villus height to crypt depth induced by magnolol and honokiol may reduce the secretion capacity to downregulate the inflammatory cytokines and delay the apoptosis process [28,29]. These results verify our findings that magnolol and honokiol enhanced the anti-inflammatory function to promote the intestinal barrier and regulate the intestinal epithelium apoptosis.

Conclusions

In summary, in the diarrhea mice, intraperitoneal administration of ETEC induced inflammation, disrupting the ileum intestinal function and causing damage. Administration of different doses of magnolol and honokiol inhibited the mRNA expression of inflammatory cytokines and elongated the villus height and crypt depth, decreased the goblet cells numbers and the

ratio of villus height to crypt depth, and inhibited the intestinal epithelium apoptosis, effectively protecting the intestinal mucosal integrity to regulate the intestinal dysfunction.

Conflicts of interest

None.

References:

- Lucas ML: Diarrhoeal disease through enterocyte secretion: A doctrine untroubled by proof. *Exp Physiol*, 2010; 95(4): 479–84
- Johnson AM, Kaushik RS, Rotella NJ, Hardwidge PR: Enterotoxigenic *Escherichia coli* modulates host intestinal cell membrane asymmetry and metabolic activity. *Infect Immun*, 2009; 77(1): 341–47
- Kim JM, Eckmann L, Savidge TC et al: Apoptosis of human intestinal epithelial cells after bacterial invasion. *J Clin Invest*, 1998; 102(10): 1815–23
- Wu SG, Lim KC, Huang J et al: Bacteroides fragilis enterotoxin cleaves the zonula adherens protein, E-cadherin. *Proc Natl Acad Sci USA*, 1998; 95(25): 14979–84
- Kopic S, Geibel JP: Toxin mediated diarrhea in the 21st century: The pathophysiology of intestinal ion transport in the course of ETEC, V-cholerae and rotavirus infection. *Toxins*, 2010; 2(8): 2132–57
- Sherman PM, Mitchell DJ, Cutz E: Neonatal enteropathies: Defining the causes of protracted diarrhea of infancy. *J Pediatr Gastr Nutr*, 2004; 38(1): 16–26
- Knight PA, Brown JK, Pemberton AD: Innate immune response mechanisms in the intestinal epithelium: Potential roles for mast cells and goblet cells in the expulsion of adult *Trichinella spiralis*. *Parasitology*, 2008; 135(6): 655–70
- Shen JL, Man KM, Huang PH et al: Honokiol and magnolol as multifunctional antioxidative molecules for dermatologic disorders. *Molecules*, 2010; 15(9): 6452–65
- Park J, Lee J, Jung ES et al: *In vitro* antibacterial and anti-inflammatory effects of honokiol and magnolol against *Propionibacterium* sp. *Eur J Pharmacol*, 2004; 496(1–3): 189–95
- Kim DW, Ko SM, Jeon YJ et al: Anti-proliferative effect of honokiol in oral squamous cancer through the regulation of specificity protein 1. *Int J Oncol*, 2013; 43(4): 1103–10
- Cho SY, Lee JH, Bae KH et al: Anti-gastritic effects of magnolol and honokiol from the stem bark of *Magnolia obovata*. *Biomolecules & Therapeutics*, 2008; 16(3): 270–76
- Qiang LQ, Wang CP, Wang FM et al: Combined administration of the mixture of honokiol and magnolol and ginger oil evokes antidepressant-like synergism in rats. *Arch Pharm Res*, 2009; 32(9): 1281–92
- Il Jeong S, Kim YS, Lee MY et al: Regulation of contractile activity by magnolol in the rat isolated gastrointestinal tracts. *Pharmacol Res*, 2009; 59(3): 183–88
- Deng YL, Han XF, Tang SX et al: Magnolol and honokiol regulate the calcium-activated potassium channels signaling pathway in Enterotoxigenic *Escherichia coli*-induced diarrhea mice. *Eur J Pharmacol*, 2015; 755: 66–73
- Sun XY, Spencer AU, Yang H et al: Impact of caloric intake on parenteral nutrition-associated intestinal morphology and mucosal barrier function. *J Parenter Enteral Nutr*, 2006; 30(6): 474–79
- Hoffman RA, Zhang GS, Nussler NC et al: Constitutive expression of inducible nitric oxide synthase in the mouse ileal mucosa. *Am J Physiol*, 1997; 272(2): G383–92
- Izzo AA, Mascolo N, Capasso F: Nitric oxide as a modulator of intestinal water and electrolyte transport. *Digest Dis Sci*, 1998; 43(8): 1605–20
- Kim BH, Cho JY: Anti-inflammatory effect of honokiol is mediated by PI3K/Akt pathway suppression. *Acta Pharmacol Sin*, 2008; 29(1): 113–22
- Tian R, Tan JT, Wang RL et al: The role of intestinal mucosa oxidative stress in gut barrier dysfunction of severe acute pancreatitis. *Eur Rev Med Pharmacol Sci*, 2013; 17(3): 349–55
- Evennett NJ, Petrov MS, Mittal A, Windsor JA: Systematic review and pooled estimates for the diagnostic accuracy of serological markers for intestinal ischemia. *World J Surg*, 2009; 33(7): 1374–83
- Berenbaum F: Proinflammatory cytokines, prostaglandins, and the chondrocyte: mechanisms of intracellular activation. *Joint Bone Spine*, 2000; 67(6): 561–64
- Fu YH, Liu B, Zhang NS et al: Magnolol inhibits lipopolysaccharide-induced inflammatory response by interfering with TLR4 mediated NF-kappa B and MAPKs signaling pathways. *J Ethnopharmacol*, 2013; 145(1): 193–99
- Li MH, Kothandan G, Cho SJ et al: Magnolol inhibits LPS-induced NF-kappa B/Rel activation by blocking p38 kinase in murine macrophages. *Korean J Physiol Pharmacol*, 2010; 14(6): 353–58
- Buchman AL MA, Bhuta S, Belle M et al: Parenteral nutrition is associated with intestinal morphologic and functional changes in humans. *J Parenter Enteral Nutr*, 1995; 19(6): 453–60
- Blomgran R, Zheng LM, Stendahl O: Uropathogenic *Escherichia coli* triggers oxygen-dependent apoptosis in human neutrophils through the cooperative effect of type 1 fimbriae and lipopolysaccharide. *Infect Immun*, 2004; 72(8): 4570–78
- Flynn AN, Buret AG: Caspases-3,-8, and-9 are required for induction of epithelial cell apoptosis by enteropathogenic *E-coli* but are dispensable for increased paracellular permeability. *Microb Pathogenesis*, 2008; 44(4): 311–19
- Lundgren O: Enteric nerves and diarrhoea. *Pharmacol Toxicol*, 2002; 90(3): 109–20
- Chen HY, Hung YC, Lee EJ et al: The protective efficacy of magnolol in hind limb ischemia-reperfusion injury. *Phytomedicine*, 2009; 16(10): 976–81
- Tang XJ, Yao K, Zhang L et al: Honokiol inhibits H₂O₂-induced apoptosis in human lens epithelial cells via inhibition of the mitogen-activated protein kinase and Akt pathways. *Eur J Pharmacol*, 2011; 650(1): 72–78